Cabrera et al. (2021) Experimental and numerical analysis of preload in Extended Hollo-Bolt blind bolts. Journal of Constructional Steel Research. 186, 106885. https://doi.org/10.1016/j.jcsr.2021.106885

# Experimental and Numerical Analysis of Preload in Extended Hollo-Bolt Blind Bolts

Manuela Cabrera[a,*], Walid Tizani[a], Jelena Ninic[a], Fangying Wang[a]

[a]*Department of Civil Engineering, The University of Nottingham, Nottingham, UK*

**Abstract**

Adequate initial bolt preload is necessary to ensure the strength and stiffness of bolted connections. In this study, an experimental torque control method was used to determine the relationship between tightening torque and preload of nine Extended Hollo-Bolt (EHB) blind bolted connections to Concrete-Filled Steel Hollow Sections (CFSHS). In order to obtain the EHB nut factors, which allow to calculate the level of preload for any value of applied torque, torque versus preload curves were drawn based on the experimental results and curve fitting method was carried out. Bolt preload relaxation was also recorded for a period of 7 days while concrete hardening occurred. Additionally, a detailed 3D Finite Element (FE) model of the tightening stage of the EHB was established. The experimental and numerical results show that the nut factor for the EHB is higher than that of standard bolts and bolt relaxation is not affected by the concrete presence during the hardening stage. Adequate friction coefficients were proposed as well as an equation for calculating the residual preload of the EHB.

*Keywords:* Preload, Extended Hollo-Bolt, Blind Bolt

*Corresponding author: M. Cabrera, Email: manuela.cabrera@nottingham.ac.uk

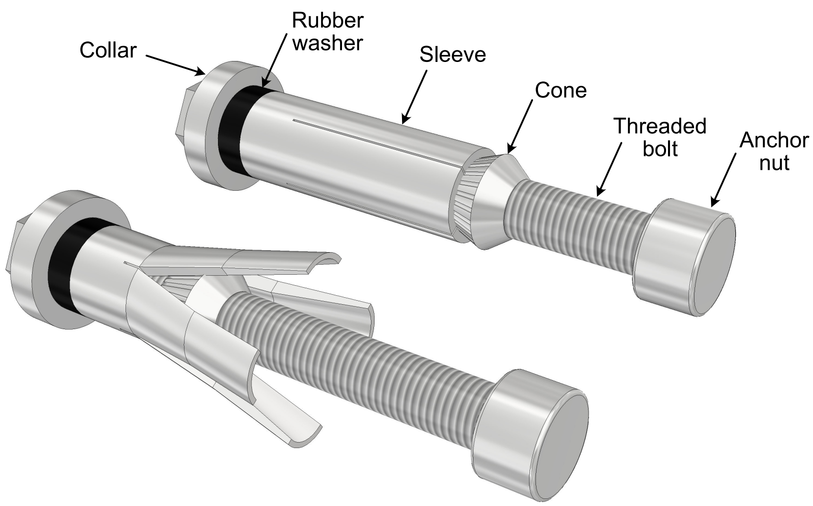


**Fig. 1.** Extended Hollo-bolt (EHB) deformed and undeformed shape.

## 1. Introduction

Blind bolted joints are used in mechanical structures as they are easy to be assembled in Steel Hollow Sections (SHS). Some commercial blind bolts are the Blind Oversized Mechanical locked bolt (BOM), the Ultra-twist, the Flowdrill bolt, the Ajax anchored blind bolt, and the Hollo-Bolt (HB). The Extended Hollo-Bolt (EHB) [1] is a modification of the HB, which has an anchor nut attached to an extended bolt shank, additionally to the five original components of the HB: cone, collar, sleeve, rubber washer and threaded bolt. The tightened shape of the EHB differs from its untightened shape as the sleeve expands while the cone is pushed up during tightening, as shown in Fig. 1. This type of fastener is the subject of an ongoing research programme at the University of Nottingham for its application in moment resisting connections [2, 3, 4].

As any threaded fastener, blind bolts are tightened when installed creating a clamping force which compresses the connected components with the purpose of strengthening the reliability of the connection [5]. The tension force caused after tightening is called the preload and it significantly affects the connection initial stiffness, plastic resistance, and component secant stiffness [6, 7]. Determining the appropriate level of preload is therefore critical, since excessive load could cause yield and fracture of the bolt while insufficient preload cannot provide the adequate clamping force required for the joint integrity.

The level of preload achieved during assembly is difficult to measure directly, hence various control methods such as torque-only, torque-turn/angle, bolt elongation, and torque-to-yield are generally used to control the preload level induced during installation [8].

This paper presents the experimental results of nine preload and relaxation tests performed in CFSHS with EHBs. It also investigates the influence of bolt diameter, and bolt grade on the preload behaviour of this type of fastener. Additionally, Finite Element (FE) models are presented to simulate the tightening process of the blind fastener and perform a parametric study.

The objectives of this work involve the proposal of an appropriate nut factor for application in the short-form equation in EHB connections, proposal of adequate friction coefficients for the long-form equation, prediction of the residual preload in the blind-bolt assembly, and identification of the concrete influence in the bolt relaxation process.

The remaining of the paper is organized as follows: Section 2 presents the available preload equations for standard bolts and the state of the art of experiments and numerical modelling of preload in blind bolts; the experimental set up and numerical model developed in the present work are described in Section 3, and their respective results are presented in Section 4 and Section 5 as well as parametric studies; Section 6 presents a summary of the coefficients proposed and modified equations that can be applied specifically to the EHB according to the findings of the present work; and finally, the conclusions and limitations of the research are presented in Section 7.

## 2. Background

### *2.1. Theoretical relation between torque and preload*

The relationship between the tightening torque and preload (tightening stage) is highly influenced by friction variations and therefore, the clamping load achieved is hardly predicted in a reliable fashion.

Motosh [9] provided a torque–preload relationship related to variables inherent to the tightened bolt, known as the long-form equation:

$$T = F_{p,ini}\left(\frac{P}{2\pi} + \frac{\mu_t r_t}{cos\beta} + \mu_b r_b\right) \tag{1}$$

Where:

T = applied torque (Nm)

$F_{p,ini}$ = initial bolt preload (kN)

P = thread pitch (mm)

$\mu_t$ = coefficient of thread friction (dimensionless)

$r_t$ = effective thread contact radius (mm)

$\mu_b$ = coefficient of underhead friction (dimensionless)

$r_b$ = effective underhead bearing contact radius (mm)

$\beta$ = half of the thread profile angle (30° for standard UN and ISO threads).

Equation 1 shows that the applied torque is resisted by three reaction torques: the bolt stretch component, produced by the inclined plane on bolt and nut threads; the thread frictional component, produced by the restraint between nut and bolt threads; and nut component, created by the frictional restraint between the face of the nut and the washer or joint. Bearing friction coefficients $\mu_b$ found in the literature vary from 0.2 to 0.45 (0.2 [10], 0.25 [11], 0.44 [12], 0.45 [3]), while thread coefficients $\mu_t$ range from 0.025 to 0.1 [13]. As expected, $\mu_t$ values are smaller than $\mu_b$ as resistance to slide mainly arises from the mechanical interlock caused by the threads geometry. The values of these coefficients vary depending on each application and therefore they are investigated in the present work specifically for the EHB.

A simplified version of the relationship above, denominated the short-form torque–preload equation [14] presented in Equation 2, is generally used for general nuts and bolts with rolled thread without lubrication.

$$T = F_{p,ini} K d_b \tag{2}$$

Where $T$ is the applied torque (Nm), $F_{p,ini}$ is the initial bolt preload (kN), $K$ is nut factor (dimensionless), and $d_b$ is the bolt nominal diameter (mm). The nut factor is an experimental coefficient that includes all factors affecting the relationship between the preload and the torque such as friction, torsion, bending, plastic deformation of threads, etc [14]. This factor is different for each application and therefore determined experimentally.

In the literature, nut factor ranges for standard bolts are found to be dependent on the materials of the connected members. An approximated value of 0.2 has been provided by various authors for typical un-lubricated mid-size steel fasteners [15, 16, 17, 18]. For blind bolts, the value of 0.3 has been used by different authors [19, 20, 21]. Discrepancies between the theoretical and experimental preload values have been reported claiming these to be caused by uncertainties over the nut factor. This is primarily owing to the fact that the clamping mechanism of each blind fastener is different to that of an standard bolt as there are usually more components interacting with each other. In the case of the EHB, the most influential interactions are in the interface between the sleeve and column tube, and between the cone and sleeve.

In terms of the HB blind fastener, Pitrakkos [22] conducted a statistical and probability analysis of the experimental nut factor obtained from 20 preload tests carried out on standard HBs. It was concluded that there is 95% probability that the nut factor for HB lies between 0.415 and 0.525. This indicates that the value of 0.2 recommended for standard bolts overestimates the HB preload, and higher K values are anticipated for this kind of fasteners as the magnitude of preload developed in a HB assembly is lower than that of a standard bolt. Consequently, it is necessary to obtain an accurate nut factor for specific blind bolted connections by appropriate experiments in critical applications. Regarding the EHB blind fastener, there is no experimental information regarding the nut factor in the literature, therefore it is the purpose of this work to establish experimentally and numerically the relationship between torque and initial preload.

### 2.2. Preload Relaxation

After tightening, the bolt preload experiences losses, which is termed as relaxation (casting and hardening stages). The relaxation rate is rapid at the beginning and reduces over time for standard bolts. In the short term, the reduction in the initial preload is caused mainly by embedment processes. This process includes readjustment of the members surfaces after the first contact as they are not perfectly flat or elastic recovery of components, plastic deformation due to poor thread engagement or non perpendicular bolt heads, irregular stress distribution due to joint members bending, etc [14].

Pitrakkos and Tizani [23] reported experimental results for 20 preload tests carried out on HB to measure the relaxation effects over a five days period. Overall, the general pattern of preload relaxation is in agreement with the standard bolts graph. The authors concluded that at least 90% of bolt relaxation occurs within two hours of tightening.

In the case of the EHB connection, the concrete hardening and the bolt relaxation occur simultaneously. The influence of concrete hardening on EHB relaxation are yet to be explored; the present study is therefore aiming at addressing this.

### 2.3. Finite Element Analysis

Finite Element Analysis (FEA) is a reliable and widely used method to simulate complex bolted connections. Different authors have used detailed 3D FE models to simulate bolt tightening in a wide range of applications by adopting various modeling techniques. For instance, Hwang [24] modeled a joint in vehicle design process based on torque–angle curves. The relationship between torque and preload was found by applying a torque gradually and comparing it to the achieved preload, and the numerical results were validated with experiment results. Ganeshmurthy and Nassar [13] considered the detailed thread geometry taking into account the helix angle under different torque-only and torque-turn methods which are commonly used for automating the assembly of bolted joints in a mass production environment. The stress distribution on the threads due to axial loading in joints with parallel and nonparallel bearing surfaces were investigated. The authors found that the results from torque-only simulations are in good agreement with theoretical values and this control method is more reliable than the torque-angle strategy. The general pre-tightening process of bolted joints was studied by Yu et al. [5] who compared the relationship between the torque and initial preload with values calculated from theoretical equations. Additionally, the authors studied the influence of a range of key parameters on the relationship, including the friction coefficient, pitch, elastic modulus, assembly clearance, and strain-hardening exponent. The developed model showed good agreement with theoretical results when predicting the relation of tightening torque and initial load.

The aforementioned studies have shown that numerical simulations can be used to determine torque settings numerically, for a wide range of applications, and can be developed as a standard practice for determining joint torque when designing joints. Therefore, it was employed in this study to model the EHB preload.

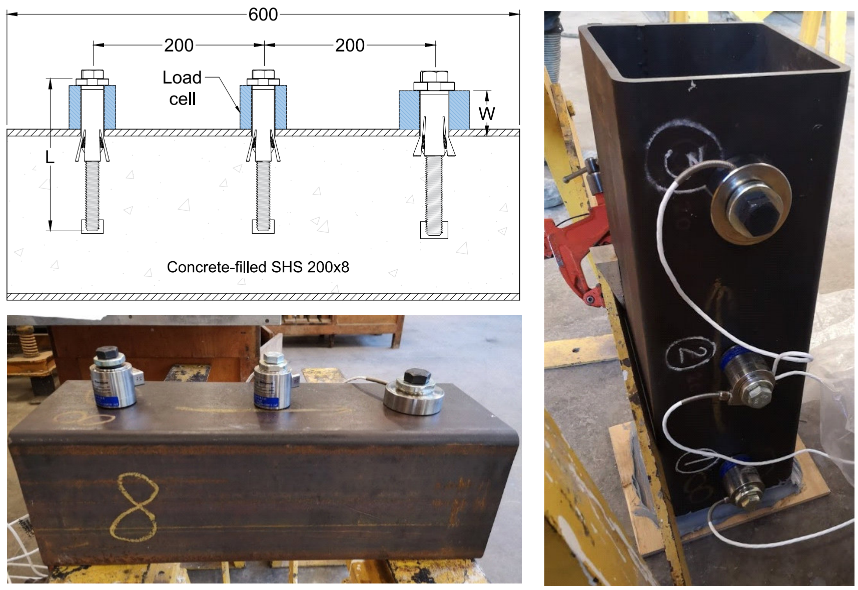


**(a)** Tightening position **(b)** Casting position

**Fig. 2.** Preload test set up.

## 3. Experimental and numerical programme

### *3.1. Test setup*

A total of nine tests were performed to measure the preload levels that are induced in the EHBs during tightening. Three batches of tests were carried out, each comprising three 150mm bolt shank EHBs tested simultaneously to ensure consistency in the concrete batch. The specimen indexes are defined in the current work as: EHB(1)-(2)-(3), where (1) Bolt diameter, (2) Bolt

**Table 1.** Preload tests parameters.

| Specimen | Bolt diameter $d_b$ (mm) | Bolt grade | Sleeve length (mm) | Clamping W (mm) | Tightening Torque (Nm) |
|---|---|---|---|---|---|
| EHB16-8.8-1 | 16 | 8.8 | 84 | 59 | |
| EHB16-8.8-2 | 16 | 8.8 | 84 | 59 | 190 |
| EHB16-8.8-3 | 16 | 8.8 | 84 | 59 | |
| EHB16-10.9-1 | 16 | 10.9 | 84 | 59 | |
| EHB16-10.9-2 | 16 | 10.9 | 84 | 59 | 300 |
| EHB16-10.9-3 | 16 | 10.9 | 84 | 59 | |
| EHB20-8.8-1 | 20 | 8.8 | 76 | 46 | |
| EHB20-8.8-2 | 20 | 8.8 | 76 | 51 | 300 |
| EHB20-8.8-3 | 20 | 8.8 | 76 | 46 | |

grade[1], and (3) Sample number. This experimental study uses two bolt diameters M16 & M20, and two bolt grades 8.8 & 10.9 which are typical in structural applications. The details of the tested variables are listed in Table 1.

The test setup displayed in Fig. 2 consists of a SHS with three pre-drilled holes to install the EHBs, load cells (130 - 220 kN load capacity) with central holes to accommodate the bolts, and concrete. A torque control system, as recommended by the HB maker, was utilised at arbitrary intervals of 10

[1]The property class is given by two numbers separated by a dot. The first number indicates 1/100 of the nominal tensile strength in MPa, and the second number represents 10 times the ratio between the nominal yield strength and the nominal tensile strength [25].

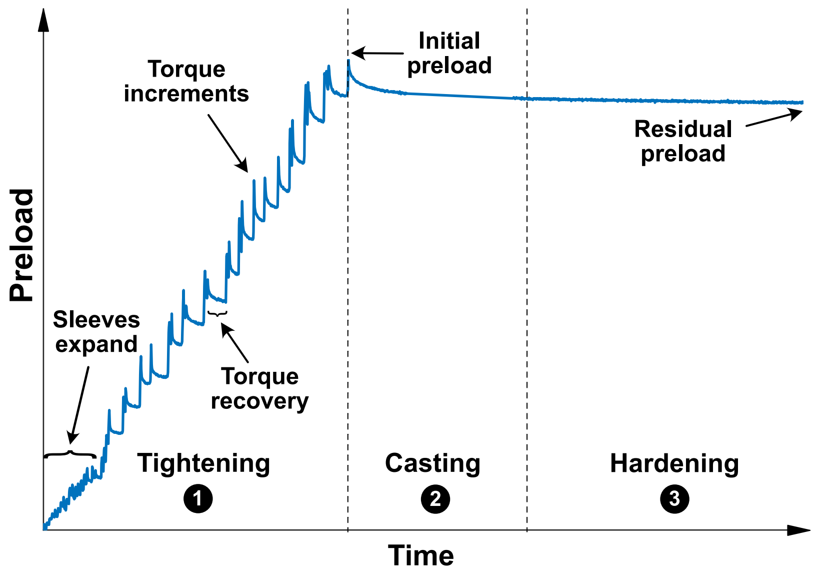


**Fig. 3.** EHB preload test stages (not to scale).

and 20Nm up to the recommended torque levels of 190 and 300 Nm, for HB M16 and M20, respectively [26]. The load cells were used to record the correspondent induced preload for each torque increment during bolt tightening as well as during relaxation.

The concrete strength was measured by means of cube compressive testing at three, seven and 28 days after casting.

Fig. 3 shows the general preload trend of the EHBs over time. This can be split into three stages:

1. Tightening stage: the torque was applied gradually until the required value was achieved. Since the torque was applied manually, there is a recovery after each torque increment. During this stage, the EHB sleeves expand until clamping the connected members.

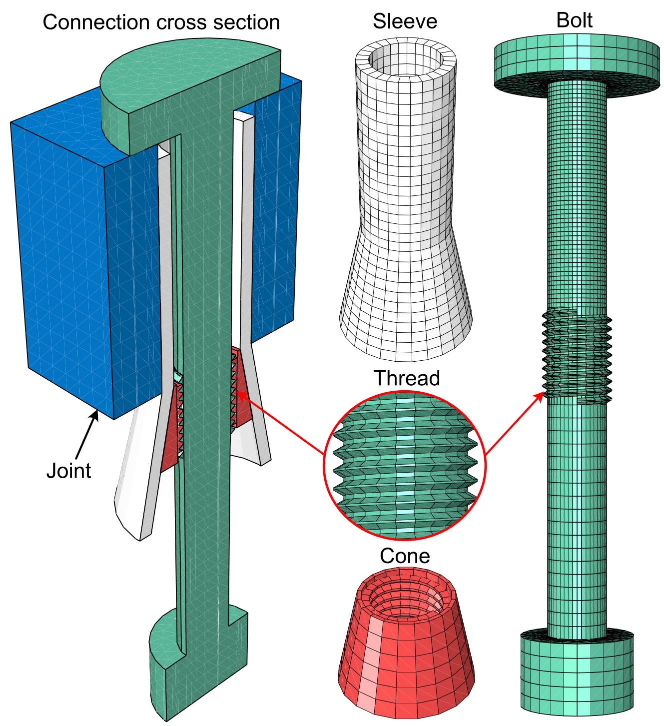


**Fig. 4.** FE connection cross section and model parts

2. Casting stage: this stage is defined in Fig. 3 from the final torque peak (initial preload) up to the point when the SHS is completely filled with concrete. This stage was monitored to see if casting and vibration would have any effect on the preload readings.

3. Hardening stage: after casting, concrete hardens while the bolts relax. The preload was recorded for a period of seven days. This zone in Fig. 3 shows the reduction of initial preload up to the residual value where changes in preload levels are negligible.

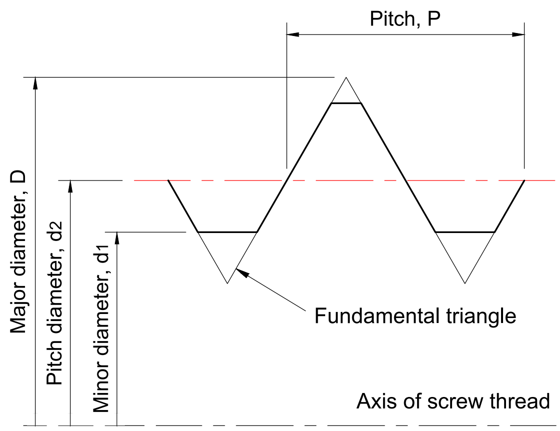


**Fig. 5.** Basic screw thread dimensions.

### *3.2. Numerical model*

3D FE models were developed to simulate the tightening process of the EHB blind bolt to further investigate the relationship between the tightening torque and initial preload. The finite element software package ABAQUS/CAE [27] was chosen to perform numerical investigation.

The FE models consists of a bolt with shank length of 150mm, a cylindrical anchor nut, a sleeve, a cone, and a joint, as shown in Fig. 4. Note that the load cell and SHS section used in the experimental setup were simulated by the joint to simplify the modelling.

The detailed thread geometry for both bolt shank and cone were used in the model. The screw thread was constructed through rotating the thread profile in Fig. 5 around the bolt and cone axis respectively. Thread dimensions were used in accordance with ISO724:1993 [28]. The thread geometry was only considered in the contact area between cone and bolt, the rest of the bolt shank was simplified as a cylinder to reduce computational processing

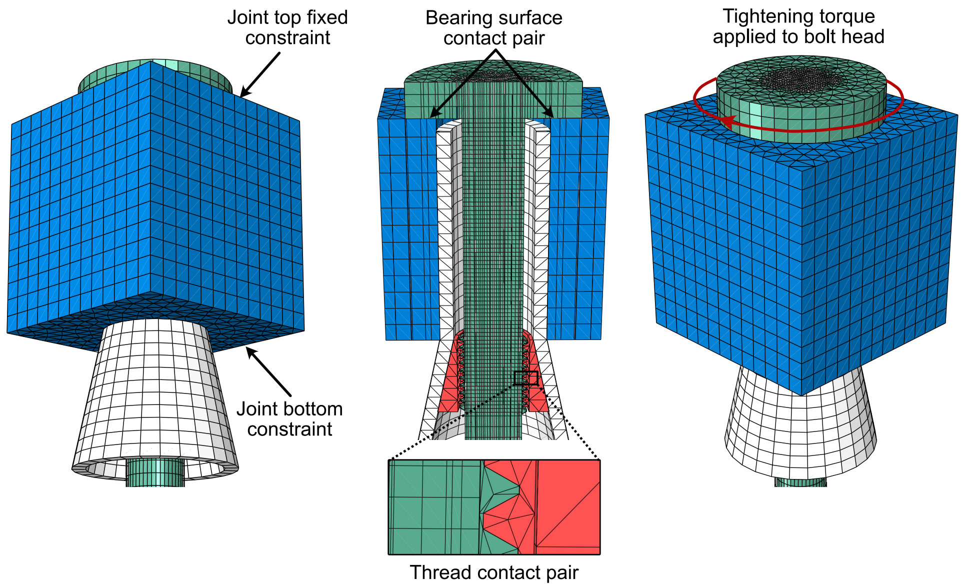


**(a)** Boundary conditions **(b)** Contact pairs **(c)** Load

**Fig. 6.** FE constrains, contacts and load.

time.

### *3.2.1. Material properties and mesh*

Elastic and plastic properties of steel based on class 10.9 fastener material were assigned to all the bolt components. Young's modulus of 210 GPa, Poisson ratio of 0.3, and density of 7.9g/cm$^3$ were considered in the material definition.

6-node linear triangular prism elements (C3D6) are used to mesh all components of the model. Different mesh sizes were assigned to different components of the FE models so as to achieve simulation accuracy while retain computational efficiency. Fine mesh (1mm element size) was used in threads and bolt shank whereas other regions were meshed with coarser elements

(3mm element size). A prior mesh convergence study was carried out in order to identify the most efficient mesh settings in terms of processing time and accuracy. The model consisted of total of 44646 linear wedge elements using type C3D6.

### *3.2.2. Boundary conditions, contacts interactions and load*

All displacements and rotations were restrained at the top surface of the joint, while the bottom surface was restrained in the lateral direction but not along the bolt axis direction. This allows the bottom surface of the joint to move along the bolt axis during the tightening process while it is compressed by the bolt (Fig. 6a). In order to reduce computation time, all model components were assumed to be in complete contact before loading.

Contact interactions were defined between all the sliding surfaces, including interfaces between bolt and cone threads, cone and sleeve, bolt collar and joint, and sleeve and joint. The default linear penalty method was used with hard contact definition for normal behaviour and friction coefficient for tangential behavior. The surface-to-surface contact pair algorithm was used for all the interactions, the effect of friction coefficients on the torque–preload relationship was investigated using sensitivity analysis, see Section 5.2.

Two contact interactions are present in the EHB connection, the bearing friction which occurs between steel-steel flat surfaces (i.e. Bolt head and joint, and sleeve and joint), and thread friction between bolt and cone threads, see Fig. 6b.

The torque was applied by assigning a moment to the bolt, as illustrated in Fig. 6c. The applied moment rotates the bolt head about its axis until torque value reaches the required torque level.

## 4. Experimental results and discussion

### 4.1. Torque-preload relationship

The applied torque versus recorded load curves for all test samples are presented in Fig. 7. Theoretically, a linear relationship is expected between the load and torque [14]. Some dispersion is observed between identical samples, which could be caused by the handheld torque wrench in the tightening process which, according to Bickford [14], has a level of accuracy of ±30%. The highest dispersion was found for sample EBH20-8.8 which suggests that the difference in the clamping thickness has an influential effect in the initial preload value. As specimen EHB20-8.8-2 differs significantly from the other two specimens, the results were reported but not considered in the analysis.

The mean values of initial preload are plotted against the ratio between applied torque and bolt diameter ($\mathrm{T/d_b}$) in Fig. 7d. Linear regression using least squares was carried out to find the best fit line for the experimental data, the slope of this line is $Kd_b$, and the nut factor can be calculated through Equation 3. A K value of 0.37 was found for the EHB with respect to the range of the investigated parameters.

$$K = \frac{\Delta T}{F_{p,ini} d_b} \tag{3}$$

The obtained nut factor the EHB specimens is higher than the suggested value (0.2) for typical un-lubricated mid-size steel fasteners. This is essentially attributed to the fact that there are more sources of friction in the EHB connection such as contact between sleeve and SHS, and cone and sleeve, which do not exist in a connection with a normal bolt.

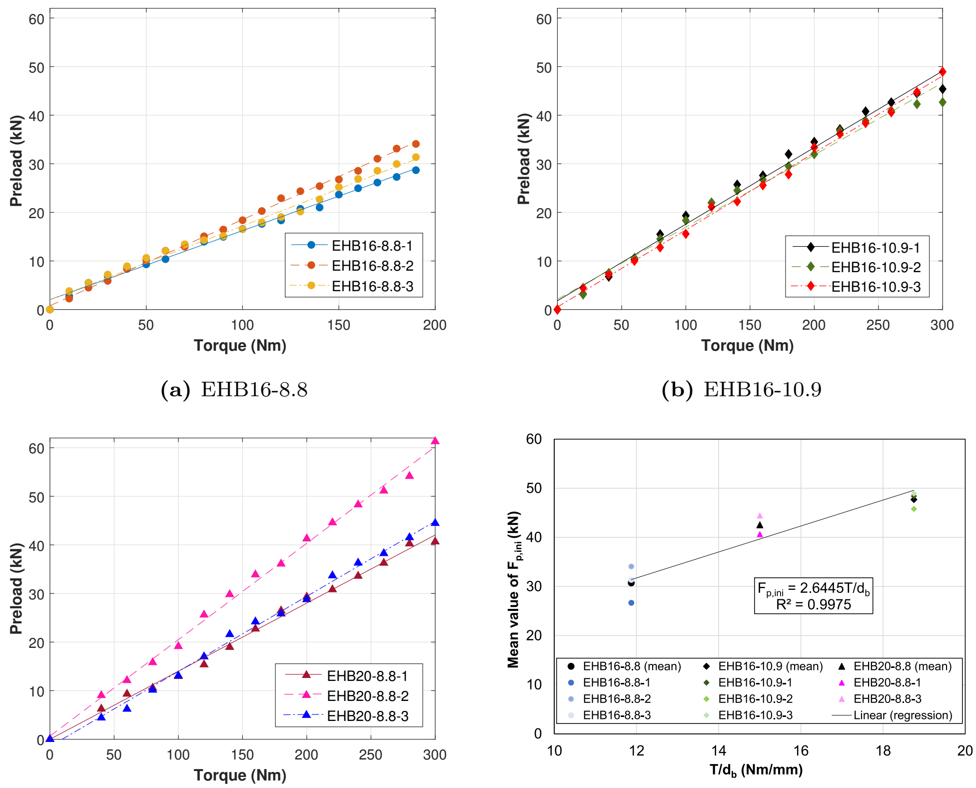


**(a)** EHB16-8.8

**(b)** EHB16-10.9

**(c)** EHB20-8.8

**(d)** Initial preload versus $T/d_b$ ratio.

**Fig. 7.** Experimental torque-preload curves for all test specimens.

**Table 2.** Initial vs residual bolt preload.

| Specimen | Preload (kN) | | | Loss (%) | | Relaxation |
|---|---|---|---|---|---|---|
| | $F_{p,ini}$ | $F_{p,24hr}$ | $F_{p,res}$ | Total | 24hr | in 24hr (%) |
| EHB16-8.8-1 | 26.7 | 21.8 | 20.9 | 21.6 | 18.2 | 84.4 |
| EHB16-8.8-2 | 34.0 | 30.0 | 28.5 | 16.5 | 12.1 | 73.5 |
| EHB16-8.8-3 | 31.4 | 27.5 | 26.1 | 17.1 | 12.5 | 73.1 |
| EHB16-10.9-1 | 45.5 | 43.2 | 43.1 | 5.0 | 5.1 | 100.0 |
| EHB16-10.9-2 | 42.6 | 38.1 | 37.3 | 12.5 | 10.6 | 84.6 |
| EHB16-10.9-3 | 48.9 | 37.5 | 35.4 | 15.9 | 10.7 | 67.5 |
| EHB20-8.8-1 | 40.7 | 38.3 | 37.8 | 7.2 | 5.9 | 81.1 |
| EHB20-8.8-2 | 61.6 | 54.7 | 53.9 | 12.4 | 11.2 | 90.3 |
| EHB20-8.8-3 | 44.5 | 37.6 | 35.3 | 20.6 | 15.4 | 75.0 |

### *4.2. Initial preload and relaxation*

The load values obtained from the experimental tests are shown in Table 2. The total loss was calculated as the percentage difference between the initial and the residual values.

After reaching the initial preload, bolt relaxation occurs over the whole connection life time. It is generally accepted that most losses occur within the first period of time after applying the torque, and stabilise over time to a residual value $F_{p,res}$. In the present work, the load was monitored for a period of seven days, beyond which the relaxation is considered to be negligible. The load recorded 24 hours after tightening ($F_{p,24h}$) was also used for the analysis.

The mean preload relaxation pattern measured over a 24-hour period for the three samples is displayed in Fig. 8a for illustration purposes. It was

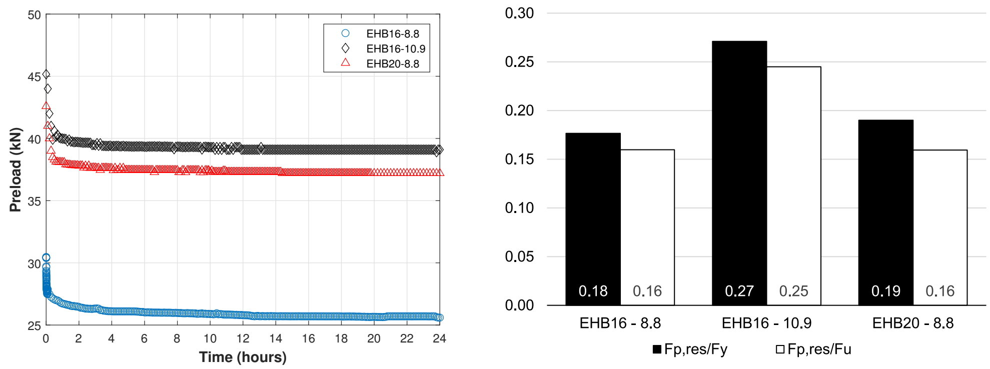


**(a)** Mean preload relaxation over first 24hr

**(b)** Normalised residual preload.

**Fig. 8.** Mean initial and residual preload analysis curves.

found that for all specimens at least 67.5% of the losses occur in the first 24 hours after reaching the initial preload, and the rate of relaxation significantly reduces thereafter.

To stablish the influence of changing bolt diameter and grade, the residual preload values were normalised with respect to the mechanical properties of the internal bolts, the mean results are displayed in Fig. 8b, where $F_y$ and $F_u$ are the bolt yield and ultimate load capacities, respectively. The bar chart shows that the relative level of residual preload in specimens EHB16-8.8 and HB20-8.8 is not influenced by the bolt diameter variation. On the other hand, varying the bolt grade from 8.8 to 10.9 produces an increase of around 46% in the level of residual preload.

### *4.3. Effect of concrete in EHB relaxation*

The effect of concrete hardening during bolt relaxation is analysed during the hardening stage. Results from the EHB experiments are presented along with HB tests values obtained by Pitrakkos [22] in Fig. 9. The graph shows

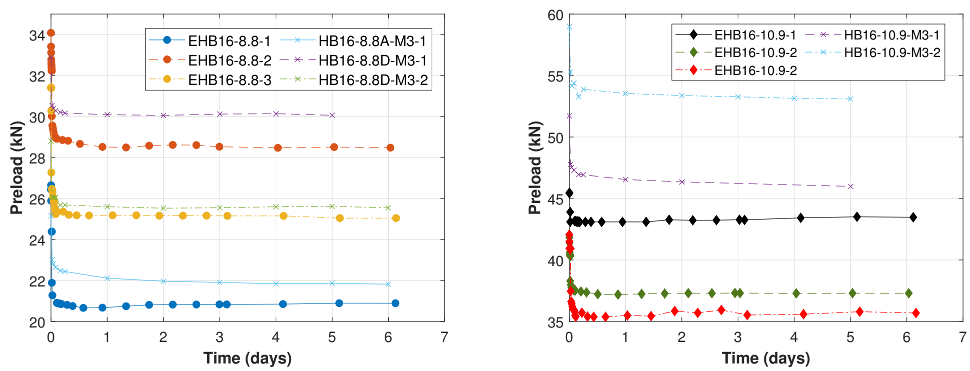


**(a)** M16-8.8 samples **(b)** M16-10.9 samples

**Fig. 9.** EHB and HB load relaxation curves.

the general trend of the EHB relaxation to be similar to that of the HB.

The 67.5% losses reached after 24 hours of tightening differs from experimental results reported by Pitrakkos and Tizani [23], where at least 90% of pre-load relaxation was reported to take place 2 hours after tightening. This suggests a delay in the load relaxation for the tested EHB in comparison with the HB. Even though there is a delay in relaxation, the relaxation patterns are similar and the effect of concrete hardening is considered negligible for the tested specimens.

## 5. Numerical results and discussion

### *5.1. Model validation*

Test samples EHB16-10.9-1, 2 & 3 showed the lowest dispersion between load measurements and therefore, they were used for the validation of the FE models. The equivalent stress distribution was monitored during the validation process. Fig. 10 shows that the maximum stress occurs at the

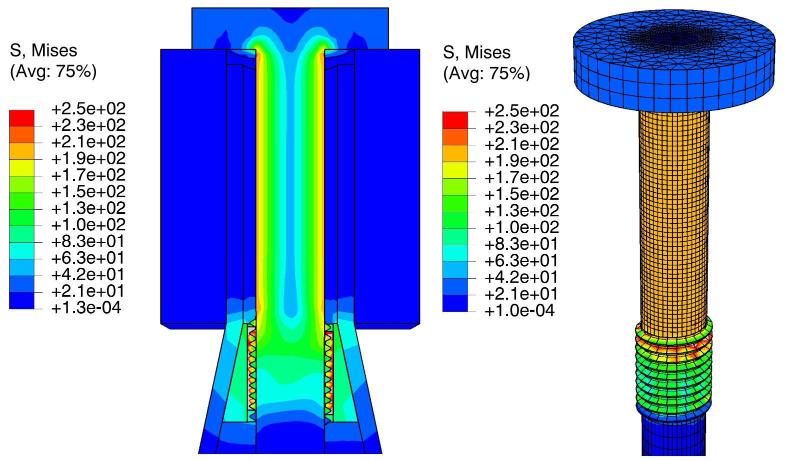


**(a)** Equivalent stress in connection (MPa) **(b)** Equivalent stress in bolt (MPa)

**Fig. 10.** FEA equivalent stress and contact contours at the end of pre-tightening process.

root of the first engaged thread which mirrors the findings from Yu et al. [5].

Equivalent stress distributions over the bolt cross section were obtained from the FE model up to a torque of 300 Nm. The load values were extracted at different tightening torques, and torque–load curves were obtained and compared with the experimental results.

The best linear fit curve for experimental results was used for validation of the numerical model. The torque-load curves corresponding to experimental and numerical results are displayed in Fig. 11a along with an error band of 10%. The torque-preload relationship was observed to be linear with a parabolic deviation up to a torque level of about 10% of the total applied torque. Good level of accuracy between numerical and experimental results was observed in the linear region of the graph. The numerical non-linear behaviour and the test curve fit deviation form value (0,0) could be caused by the free run-down stage when the nut and sleeve are adjusting during

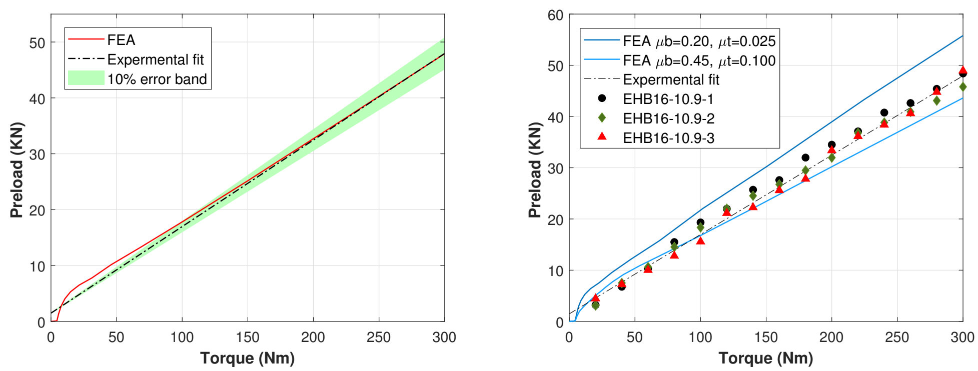


**(a)** Experimental fit vs numerical results

**(b)** Friction limits for numerical analysis

**Fig. 11.** Numerical validation for samples EBH16-10.9-1, 2 & 3

the tightening process, and by the change of frictional area caused by the expansion of the EHB sleeves.

A parabolic deviation has also been observed by Liu et al. [18] up to a torque level of 20%, the authors attributed this behaviour to deflection of the bearing surfaces which increases the friction torque. Ganeshmurthy and Nassar [13] identified two zones in the torque–preload relationship for nonparallel contact joints; the first zone ends at about 15% of the total torque and it is justified by the fact that the wedge angle is consumed by the rotated bolt head at the beginning of tightening. Gao et al. [29] also reported non-linear behaviour in the turn-preload curves up to a value of 15% of the applied turning angle. The mechanism for this effect is not completely understood, however, its effects are generally neglected as this occurs at low tightening levels.

### *5.2. Friction coefficient sensitivity analysis*

In bolted joints, the coefficient of friction determines the torque resistance to overcome the frictional forces and therefore influences the total value of the initial preload [5]. FE simulations were generated using the combination of the maximum and minimum friction coefficients found in the literature in order to give recommendations on what values are suitable for the EHB. As shown in Fig. 11b, most of the experimental results fall within these ranges justifying their use as limits for the sensitivity analysis. Values outside these ranges fall further away from the experimental nut factor and level of preload, and therefore they are not considered in the analysis.

The Morris sampling method [30] was used to generate 50 random samples within the ranges $\mu_b$ [0.20-0.45], and $\mu_t$ [0.025-0.1], and numerical analyses were performed to calculate the nut factor and initial preload. Three sensitivity analysis methods were used to rank the influence of the friction coefficients in the nut factor response: the mean of the distribution of the absolute values of the elementary effects $\mu^*$ [31], Kendall's $\tau$ [32], and Spearman's $\rho$ [33] correlation measures. High values of $\mu^*$, and values of $\tau$ and $\rho$ close to 1 indicate strong correlation with the investigated variable.

Table 3 shows that all sensitivity measures rank the thread friction $\mu_t$ as the most influential parameter meaning that there is a strong correlation between thread friction and nut factor.

In order to propose suitable values of friction coefficients for the EHB, the effect of both the bearing and thread friction coefficients on nut factor and initial preload are plotted in Fig. 12a and Fig. 12b, respectively. Contour lines drawn at K = 0.37, and at $F_{p,ini}$=46.7 kN (as per the best linear fit

**Table 3.** Parameter sensitivity measures of friction coefficients to the nut factor.

| | | Sensitivity measure of | |
|---|---|---|---|
| Method | | Bearing friction $\mu_b$ | Thread friction $\mu_t$ |
| Morris | $\mu^*$ | 0.073 | 0.137 |
| Kendall | $\tau$ | 0.174 | 0.848 |
| Spearman | $\rho$ | 0.241 | 0.953 |

to the experimental results), represent the possible combination of friction coefficients $\mu_b$ and $\mu_t$ that would produce the desired levels of load and nut factor from the FE model. An approximation has been conducted by finding the best linear fit to these contour lines and minimizing the percentage error between calculated from FEA and expected K and $F_{p,ini}$. The calculated coefficient values are $\mu_b = 0.298$ and $\mu_t = 0.044$, which produce errors of 0.65% for initial preload, and 2.59% for nut factor. Both error percentages are bellow 12%, which is considered an adequate level of accuracy for FEA of EHB connections by Mahmood [34], and therefore these friction coefficients are considered suitable and used for parametric studies.

### *5.3. Parametric study*

In this section, a series of parametric studies is presented in which the influence of the bolt grade and bolt diameter is investigated using the validated model developed in the previous section.

Samples include validation, verification, and testing sets; the validation set (Val) corresponds to the sample used to calibrate the FE model; verifica-

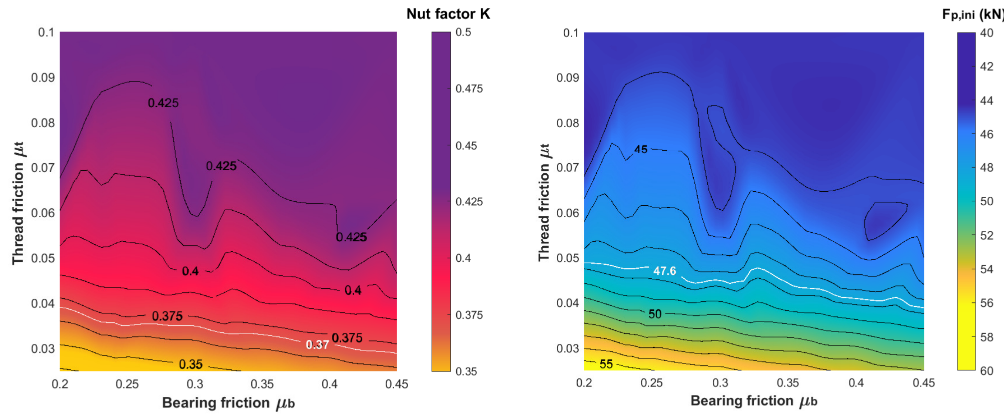


**(a)** Nut factor variation

**(b)** Initial preload variation

**Fig. 12.** Friction coefficients effect on (a) Nut factor and (b) Initial preload.

tion set (Ver) include samples with experimental results available and were used to measure the accuracy of the model; finally, the testing set (Test) was used to predict the response of samples that have not been tested. The details of the considered models is presented in Table 4 as well as the initial preload values obtained after replacing the proposed friction coefficients in the long form equation (Equation 1) for comparison. The numerical and analytical percentage error are calculated with respect to the available experimental results available.

It can be seen that numerical and analytical results for initial preload are in good agreement with the experimental results, and therefore the proposed coefficients are acceptable for the EHB blind bolt.

For the same torque level, when the bolt dimensions are reduced, less friction is expected and therefore, a higher load was observed in specimen EHB12-8.8 compared to EHB16-8.8. On the other hand, when the torque level is increased, similar load level are achieved for bolts EHB20-8.8, EHB20-

**Table 4.** Results of parametric studies.

| | | Initial preload $F_{p,ini}$ (kN) | | | Error (%) | |
|---|---|---|---|---|---|---|
| Model | Set | Exp | Num | Analyt | Num | Analyt |
| EHB16-8.8 | Val | 30.7 | 31.2 | 30.2 | -1.6 | 1.7 |
| EHB16-10.9 | Ver | 45.6 | 44.4 | 45.0 | 2.6 | 0.2 |
| EHB20-8.8 | Ver | 42.6 | 42.8 | 41.3 | -0.5 | 3.2 |
| EHB20-10.9 | Test | - | 42.0 | 41.23 | - | - |
| EHB18-8.8 | Test | - | 28.8 | 27.3 | - | - |
| EHB18-10.9 | Test | - | 49.6 | 42.1 | - | - |
| EHB12-8.8 | Test | - | 37.1 | 37.7 | - | - |
| EHB12-10.9 | Test | - | 60.1 | 59.5 | - | - |

10.9 and EHB16-10.9. Similar to the experimental results, the numerical values for the initial preload were analysed based on the torque/diameter ratio. Results displayed in Fig. 13 show that the numerical nut factor is 0.39, which is in good agreement with experimental results in Section 4.1

## 6. Proposed coefficients and modified equations

The suitability of the proposed friction coefficients was demonstrated through numerical simulation and analytical analysis, these values were rounded to $\mu_b = 0.3$ and $\mu_t = 0.04$ and substituted into the equations presented in Section 2, resulting in the following EHB initial preload equations:

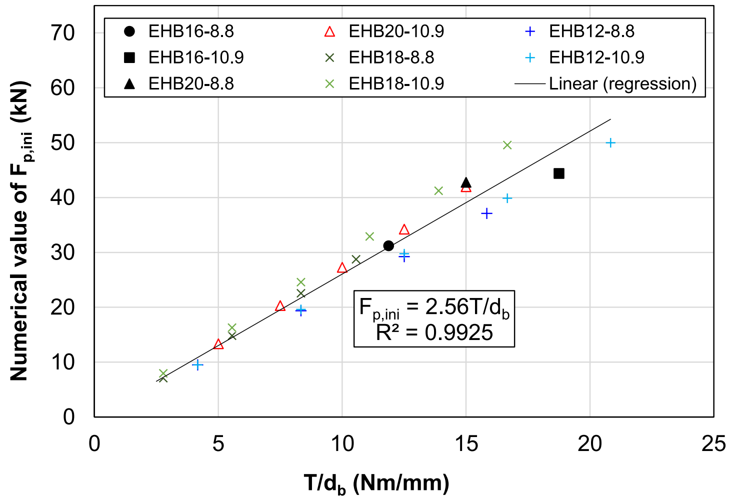


**Fig. 13.** Numerical initial preload versus T/$d_b$ ratio.

Long form equation:

$$F_{EHB,ini} = \frac{T}{(\pi^{-1} + 0.04r_t + 0.3r_b)} \tag{4}$$

Short form equation:

$$F_{EHB,ini} = \frac{T}{0.38d_b} \tag{5}$$

The maximum total loss found for the tested EHB specimens was found to be 21.6% with respect to the initial preload. The following equation is proposed for calculating the residual preload of the EHB.

$$F_{EHB,res} = 0.75F_{EHB,ini} \tag{6}$$

## 7. Conclusions

A modified blind bolt, the EHB, is under research for application in moment resisting connections. In order to fully characterize its behaviour, an experimental and numerical program was carried out to investigate the torque-preload relationship and relaxation of the EHB blind bolt for three pairs of samples varying their bolt grade and diameter for comparison. The nut coefficient was established and compared with the standard HB.

The findings of this work are restricted to EHBs with bolt diameters M12, M16, and M20 and for bolt grades 8.8 and 10.9 which are typical in structural applications using a torque control method.

The findings from this research include:

1. The concrete hardening does not influence the general relaxation pattern but it expands the time period in which most losses occur from 2 hours for HB to 24 hours for the range of studied parameters of the EHB.
2. An experimental nut factor of K=0.37 is calculated for the EHB. This shows that the typical value of K=0.2 used for un-lubricated mid-size steel fasteners is not suitable for the blind fastener as it overestimates the value of initial preload.
3. Bearing and thread friction coefficients used in the numerical model appear to have a significant effect on the torque-preload curves, where the higher the coefficients, the lower the achieved preload for the same torque value. Besides, thread coefficients are significantly lower than bearing coefficients as most resistance to bolt turn is caused by the me-

chanical interaction between the bolt and cone threads. The proposed friction values for the EHB are $\mu_b = 0.3$ and $\mu_t = 0.04$.

4. The proposed coefficients for thread and bearing frictions for FEA and analytical equations produce results that are in good agreement with experimental results.
5. After normalising the residual preload values with respect to the mechanical properties of the bolts, it was concluded that the relative level of residual preload in specimens is not influenced by the bolt diameter variation while the bolt grade variation increases the residual preload by 46%.

## 8. Acknowledgements

The authors wish to acknowledge TATA Steel, Lindapter International, and the University of Nottingham HPC, for supporting this research.

## References

[1] W. Tizani, D. J. Ridley-Elis, The performance of a new blind-bolt for moment-resisting connections, in: Tubular structures X: proceedings of the 10th international symposium on tubular structures, 2003, pp. 395–400.

[2] W. Tizani, M. Mahmood, D. Bournas, Effect of concrete infill and slenderness on column face component in anchored blind-bolt connections, The Journal of Structural Engineering 146 (2020) 04020041 1–18. doi:10.1061/(ASCE)ST.1943-541X.0002557.

[3] M. Cabrera, W. Tizani, M. Mahmood, M. F. Shamsudin, Analysis of extended hollo-bolt connections: Combined failure in tension, Journal of Constructional Steel Research 165 (2020) 105766 1–14. doi:10.1016/j.jcsr.2019.105766.

[4] M. Cabrera, W. Tizani, J. Ninic, A review and analysis of testing and modeling practice of extended hollo-bolt blind bolt connections, Journal of Constructional Steel Research 183 (2021) 106763. doi:https://doi.org/10.1016/j.jcsr.2021.106763.

[5] Q. Yu, H. Zhou, L. Wang, Finite element analysis of relationship between tightening torque and initial load of bolted connections, Advances in Mechanical Engineering 7 (2015) 1–8. doi:10.1177/1687814015588477.

[6] J.-P. Jaspart, R. Maquoi, Effect of bolt preloading on joint behaviour, in: Proceedings of the First European Conference on Steel Structures, Athens, Greece, 1995, pp. 219–226.

[7] Y. Oktavianus, H. M. Goldsworthy, E. Gad, Group behavior of double-headed anchored blind bolts within concrete-filled circular hollow sections under cyclic loading, Journal of Structural Engineering 143 (2017) 04017140 1 – 14. doi:10.1061/(ASCE)ST.1943-541X.0001882.

[8] T. Sakai, Bolted Joint Engineering: Fundamentals and Applications, Beuth Training, Beuth Verlag GmbH, 2008.

[9] N. Motosh, Development of design charts for bolts preloaded up to the

plastic range, Journal of Engineering for Industry 98 (1976) 849–851. doi:10.1115/1.3439041.

[10] S. Chen, J. Jiang, L. Jia, Numerical study on the performance of beam-to-concrete-filled steel tube column joint with adapter-bracket, Advances in Structural Engineering 21 (2018) 1542–1552. doi:10.1177/1369433217746345.

[11] A. M. Pascual, M. L. Romero, W. Tizani, Fire performance of blind-bolted connections to concrete filled tubular columns in tension, Engineering Structures 96 (2015) 111 – 125. doi:10.1016/j.engstruct.2015.03.067.

[12] G. Shi, Y. Shi, Y. Wang, M. A. Bradford, Numerical simulation of steel pretensioned bolted end-plate connections of different types and details, Engineering Structures 30 (2008) 2677–2686. doi:10.1016/j.engstruct.2008.02.013.

[13] S. Ganeshmurthy, S. A. Nassar, Finite element simulation of process control for bolt tightening in joints with nonparallel contact, Journal of Manufacturing Science and Engineering 136 (2014). doi:10.1115/1.4025830, 021018.

[14] J. H. Bickford, Introduction to the Design and Behavior of Bolted Joints, 4th ed., Yaylor & Francis Group, 2008.

[15] R. Juvinall, K. Marshek, Fundamental of machine component design, fifth ed., John Wiley & Sons, INC., 2000.

[16] S. A. Nassar, P. H. Matin, G. C. Barber, Thread friction torque in bolted joints, ASME. J. Pressure Vessel Technol 127 (2005) 387–393. doi:https://doi.org/10.1115/1.2042474.

[17] eFunda Inc, Torque and tension in bolts, 2020. URL: http://www.efunda.com/designstandards/screws/fasteners_intro.cfm.

[18] Z. Liu, M. Zheng, X. Yan, Y. Zhao, Q. Cheng, C. Yang, Changing behavior of friction coefficient for high strength bolts during repeated tightening, Tribology International 151 (2020) 106486. doi:https://doi.org/10.1016/j.triboint.2020.106486.

[19] Z. Wang, W. Tizani, Q. Wang, Strength and initial stiffness of a blind-bolt connection based on the t-stub model, Engineering Structures 32 (2010) 2505 – 2517. doi:10.1016/j.engstruct.2010.04.005.

[20] Z.-Y. Wang, Q.-Y. Wang, Yield and ultimate strengths determination of a blind bolted endplate connection to square hollow section column, Engineering Structures 111 (2016) 345 – 369. doi:10.1016/j.engstruct.2015.11.058.

[21] L. Sun, M. Liu, Y. Liu, P. Wang, H. Zhao, J. Sun, Y. Shang, Studies on t-shaped one-side bolted connection to hollow section column under bending, Journal of Constructional Steel Research 175 (2020) 106359 1 – 21. doi:10.1016/j.jcsr.2020.106359.

[22] T. Pitrakkos, The Tensile Stiffness of a Novel Anchored Blind-bolt Component for Moment-resisting Connections to Concrete-filled Hollow Sections, Ph.D. thesis, University of Nottingham, Nottingham, UK, 2012.

[23] T. Pitrakkos, W. Tizani, Experimental behaviour of a novel anchored blind-bolt in tension, Engineering Structures 49 (2013) 905 – 919. doi:10.1016/j.engstruct.2012.12.023.

[24] H. Hwang, Bolted joint torque setting using numerical simulation and experiments, Journal of Mechanical Science and Technology 27 (2013) 1361–1371. doi:10.1007/s12206-013-0317-2.

[25] ISO898-1:2013, Mechanical properties of fasteners made of carbon steel and alloy steel, International Organization for Standardization, 2013.

[26] Lindapter International, Hollo-bolt product brochure, 2019.

[27] Dassault Systemes, Abaqus analysis user's guide, version 6.14, Dassault Systemes Simulia Corp, Providence, United States, 2014.

[28] ISO724:1993, General-purpose metric screw threads - Basic dimensions, International Organization for Standardization, 1993.

[29] D. Gao, J. Gong, Z. Tian, T. Zheng, Research on bolt pre-tightening and relaxation mechanism under transverse load, Advances in Mechanical Engineering 12 (2020) 1687814020975919. doi:10.1177/1687814020975919.

[30] M. Morris, Factorial sampling plans for preliminary computational experiments, Technometrics 33 (1991) 161–174. doi:10.2307/1269043.

[31] F. Campolongo, J. Cariboni, A. Saltelli, An effective screening design for sensitivity analysis of large models, Environmental Modelling & Software 22 (2007) 1509 – 1518. doi:10.1016/j.envsoft.2006.10.004.

[32] M. G. Kendal, A new measure of rank correlation, Biometrika 30 (1938) 81–93. doi:10.1093/biomet/30.1-2.81.

[33] C. Spearman, The proof and measurement of association between two things, The American Journal of Psychology 100 (1987) 441–471. doi:10.2307/1422689.

[34] M. Mahmood, Column Face Bending of Anchored Blind Bolted Connections to Concrete Filled Tubular Sections, Ph.D. thesis, University of Nottingham, 2015.